OXIDATION OF C/SiC COMPOSITES AT REDUCED OXYGEN PARTIAL PRESSURES

E.J. Opila
NASA Glenn Research Center
Cleveland, OH

J.L. Serra*
The Pennsylvania State University
University Park, PA

ABSTRACT

T-300 carbon fibers and T-300 carbon fiber reinforced silicon carbide composites (C/SiC) were oxidized in flowing reduced oxygen partial pressure environments at a total pressure of one atmosphere (0.5 atm O_2, 0.05 atm O_2 and 0.005 atm O_2, balance argon). Experiments were conducted at four temperatures (816°, 1149°, 1343°, and 1538°C). The oxidation kinetics were monitored using thermogravimetric analysis. T-300 fibers were oxidized to completion for times between 0.6 and 90 h. Results indicated that fiber oxidation kinetics were gas phase diffusion controlled. Oxidation rates had an oxygen partial pressure dependence with a power law exponent close to one. In addition, oxidation rates were only weakly dependent on temperature. The C/SiC coupon oxidation kinetics showed some variability, attributed to differences in the number and width of cracks in the SiC seal coat. In general, weight losses were observed indicating oxidation of the carbon fibers dominated the oxidation behavior. Low temperatures and high oxygen pressures resulted in the most rapid consumption of the carbon fibers. At higher temperatures, the lower oxidation rates were primarily attributed to crack closure due to SiC thermal expansion, rather than oxidation of SiC since these reduced rates were observed even at the lowest oxygen partial pressures where SiC oxidation is minimal.

INTRODUCTION

The oxidation of carbon fibers and carbon fiber reinforced silicon carbide composites (C/SiC) have been studied extensively in oxygen or air[1-6] and in water vapor containing environments[7]. It is known that the fiber oxidation kinetics dominate the stress rupture lifetime of C/SiC material[8]. Bulk carbon oxidation has been studied in reduced oxygen partial pressures[9-10]. However, limited data are available that quantitatively describe the oxidation behavior of C/SiC composites in reduced oxygen partial pressure environments. These environments are of considerable importance for the application of C/SiC as leading edges for hypersonic vehicles which are subject to extreme heating in the upper atmosphere during re-entry. The objectives of this study are to quantify the oxidation rates of both the constituent carbon fibers as well as the C/SiC composites at high temperatures and low oxygen partial pressures, to understand the dominant oxidation mechanisms, and to provide input to a math model for C/SiC behavior in hypersonic environments[11].

---

*Undergraduate intern at NASA Glenn Research Center, summer 2007.

EXPERIMENTAL PROCEDURE

T-300 fiber was obtained as woven fabric that had been heat treated to 1538°C (2800°F). Fiber tows (1k tow) were removed from the fabric in batches of approximately 0.5g total weight. The fiber was bundled and compressed into an alumina crucible (99.8% purity) with a slotted lower surface. CVI C/SiC coupons (1538°C HTT T-300 in $(0/45/90/-45)_{2S}$ layup) of approximate dimensions 2.5 x 1.3 x 0.25 cm were obtained from GE Power Systems. Coupons were fabricated with a hole of approximately 0.25 cm diameter. All coupons were sealed with a final CVD SiC seal coat so that no carbon fiber was exposed. As expected, cracks were present in the as-fabricated coupons, both in the SiC matrix and coating, due to thermal expansion mismatch between the SiC and T-300 fibers. The oxidation kinetics of both the T-300 fibers and C/SiC coupons were monitored using the ThermoGravimetric Analysis (TGA) system shown in Figure 1. The fiber crucible or composite coupon was suspended from the microbalance with a sapphire hanger. The three test gases were purchased premixed containing 50% O_2 in Ar, 5% O_2 in Ar, or 0.5% O_2 in Ar. Experiments were conducted at one atmosphere total pressure with a gas flow rate of 100 ccm (0.4 cm/sec). For the 5% and 0.5% O_2 cases, the system was evacuated to 30 mtorr, then flushed with the test gas. This procedure was repeated three times to ensure the samples were only exposed to reduced oxygen partial pressures. Flow rates were controlled with a calibrated mass flow controller (Tylan General, RO-28, Rancho Dominguez, CA). Oxidation experiments were initiated by raising the furnace, already at temperature and equilibrated with the test gas, around a fused quartz reaction tube containing the oxidation sample. Tests were conducted at temperatures of 816°, 1149°, 1343°, and 1538°C (1500°, 2100°, 2450°, and 2800°F). Sample temperatures were obtained from a calibrated thermocouple placed directly below the suspended sample. The thermocouple was removed from the furnace after determination of the desired set point to prevent devitrification of the fused quartz reaction tubes and any effects on the SiC oxidation rate[12]. Weight change data were obtained from the Cahn 1000 microbalance (Cerritos, CA). Carbon fibers were oxidized to completion. Oxidation times varied between 0.6 and 90h. C/SiC coupons were oxidized for 25h in 0.5 atm O_2 and 100h in the reduced oxygen partial pressures. Selected C/SiC coupons were cross-sectioned and polished for optical microscopy, Scanning Electron Microscopy (SEM), and Energy Dispersive Spectroscopy (EDS).

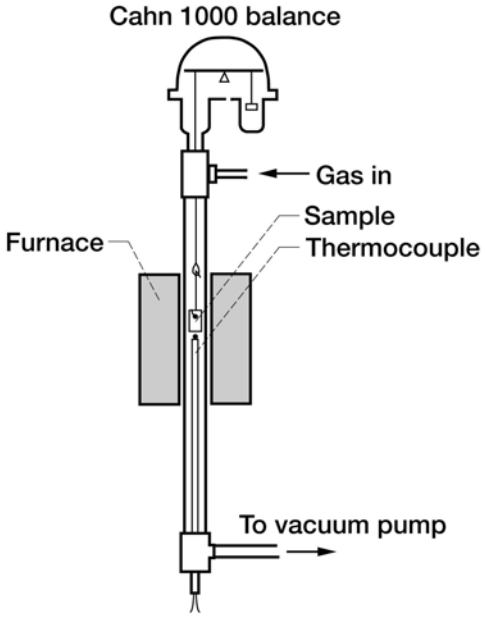

Figure 1. Schematic of Thermogravimetric Analyzer

RESULTS AND DISCUSSION

T-300 FIBER OXIDATION

Weight change data for the T-300 fibers are reported in Figures 2 through 4 as percent of initial weight. From these results it is obvious that the effect of temperature is minimal relative to the effect of oxygen partial pressure. In order to quantify the oxidation rates, the instantaneous rate at 50% fiber consumption was determined for each experiment following the procedure of Lamouroux[3]. A plot of typical instantaneous oxidation rates is shown in Figure 5. While the value at 50% consumed is reported, the observed rates were fairly constant with time (nearly linear) for all exposures. Using these rate values, the temperature and pressure dependence of the oxidation rates were evaluated. The oxidation rate temperature dependence is plotted in an Arrhenius form in Figure 6. It can be seen in comparison to the literature values of Lamouroux[2] obtained at lower temperatures, that the oxidation rates obtained here have only a weak temperature dependence. Oxidation rates obtained below 600 or 700°C appear to follow an Arrhenius relation, while those at higher temperatures do not. This is consistent with surface reaction rate controlled oxidation at lower temperatures and gas phase diffusion control at higher temperatures. From the kinetic theory of gases, gas phase diffusion is expected to have a $T^{3/2}$ dependence[13]. To determine if the oxidation rates obtained here are gas phase diffusion limited, the rates have been replotted as Log-Log in Figure 7 to determine the power law exponent for the temperature dependence. Gas phase diffusion control should result in a slope (power law exponent) of 3/2 for this type of plot. The results shown here are slightly lower than 3/2. However, due to the low number of data points and high uncertainties (95% confidence intervals reported) in the slopes, it can *not* be concluded that the temperature dependent power law exponent is statistically different from 3/2. The observed oxidation rates of T-300 fibers are therefore consistent with gas phase diffusion control.

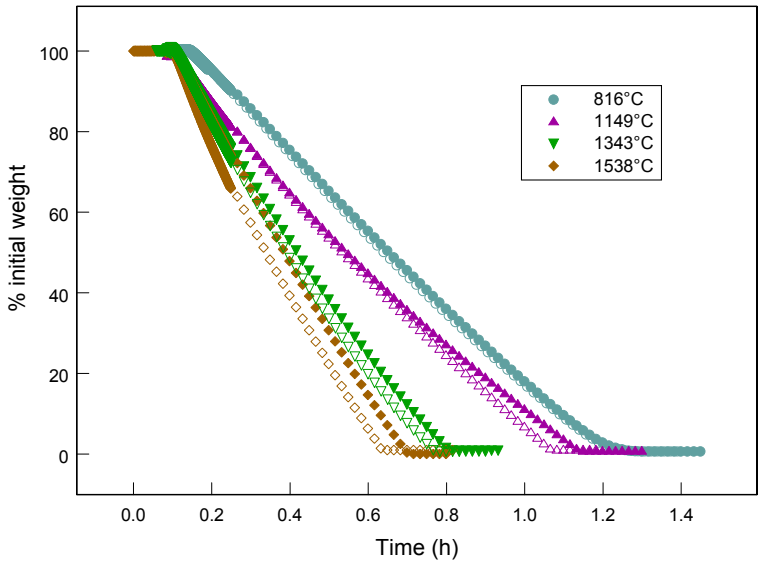

Figure 2. Oxidation weight loss of T-300 fibers in 100 ccm flowing 0.5 atm O_2/balance argon as a function of temperature.

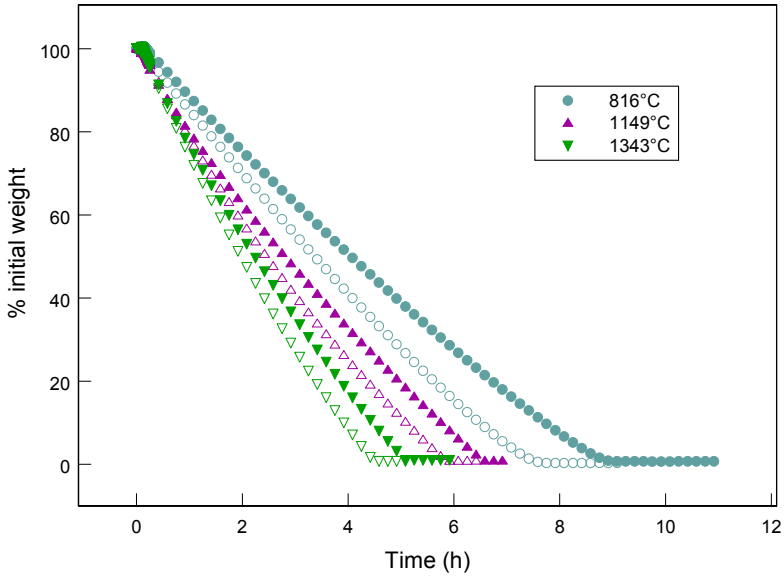

Figure 3. Oxidation weight loss of T-300 fibers in 100 ccm flowing 0.05 atm O_2/balance argon as a function of temperature.

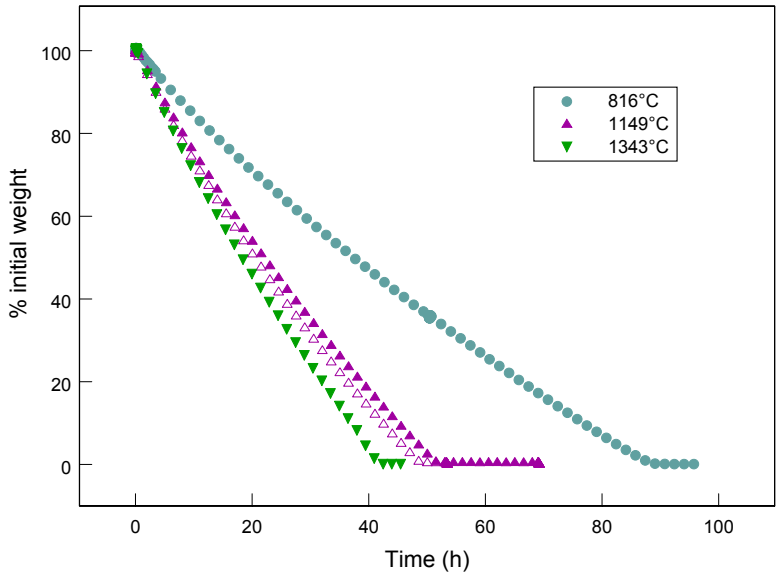

Figure 4. Oxidation weight loss of T-300 fibers in 100 ccm flowing 0.005 atm O_2/balance argon as a function of temperature.

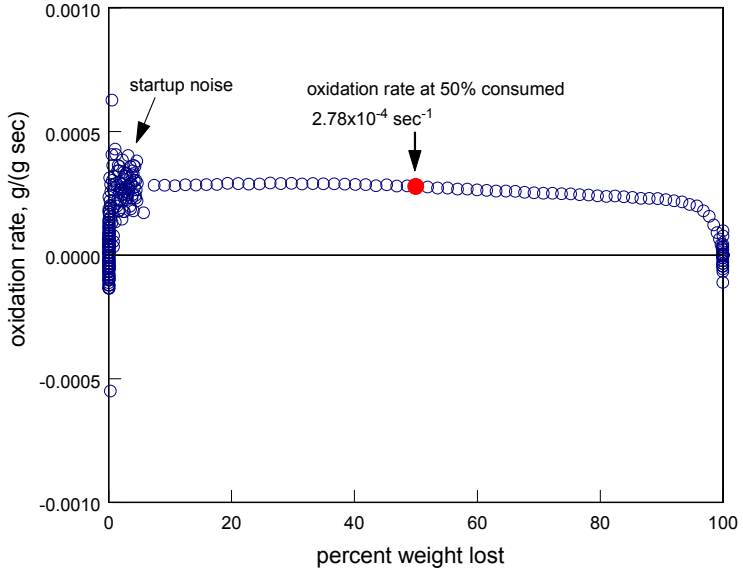

Figure 5. Instantaneous rate of oxidation rate loss for T-300 fibers exposed at 816°C in flowing (100 ccm) 0.5 atm O_2 balance argon. Reported rates obtained at 50% consumption of fibers.

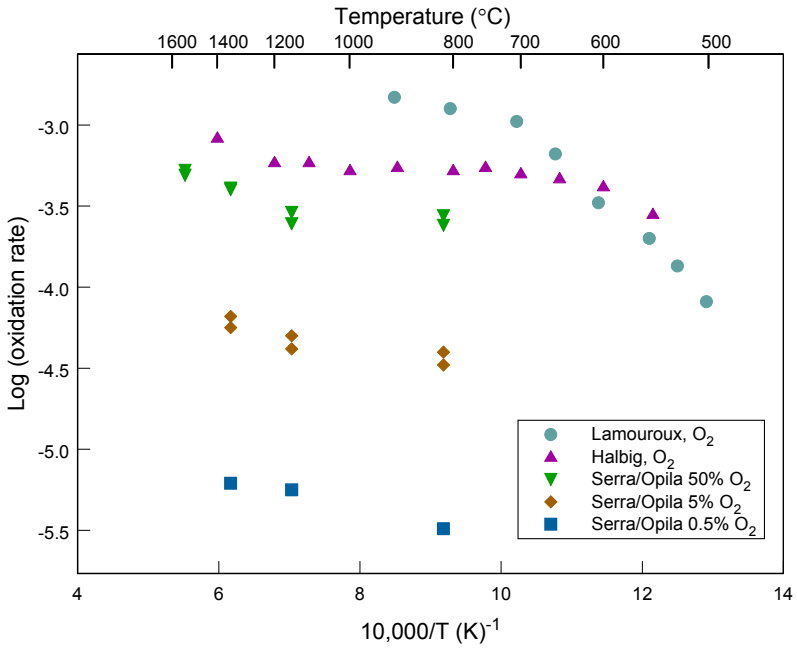

Figure 6. Arrhenius plot of T-300 fiber oxidation rates compared to values from the literature[2,5].

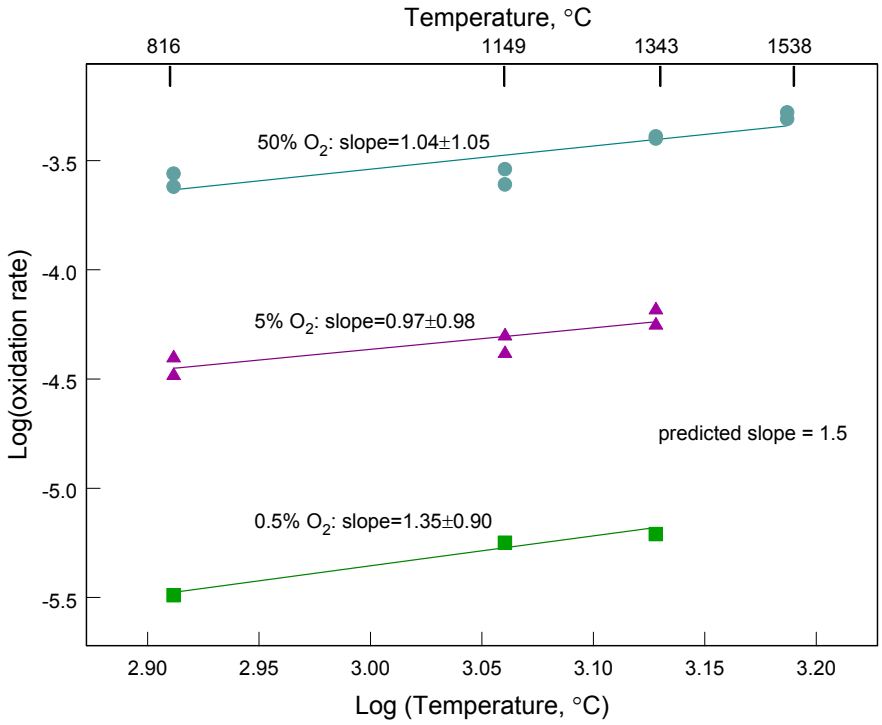

Figure 7. Power law dependence of T-300 fiber oxidation rates as a function of temperature. Predicted slope assumes gas phase diffusion controlled oxidation.

Figure 8 shows the strong variation in the weight loss results as a function of oxygen partial pressure. The pressure dependent power law exponent is determined in Figure 9, this time including data from Halbig[5] obtained at one atmosphere oxygen pressure in the same laboratory conditions as used in this study. Power law exponents approaching one are observed. This value is also consistent with gas phase diffusion control as given by the expression for the mass transfer coefficient in a gas boundary layer[14].

C/SiC COUPON OXIDATION

Weight change data for the C/SiC composites are shown in Figures 10 through 12. Weight loss is observed in all cases but one exposure at 1343°C in 50% O_2 that showed less than 1 mg weight gain. Weight change is attributed to the sum of weight loss due to carbon oxidation and weight gain due to SiC oxidation to form SiO_2. Because weight loss is almost always observed, carbon oxidation clearly dominates the observed oxidation kinetics. Ingress of oxygen through cracks in the as-processed SiC seal coat dominates the oxidation behavior. The variability in oxidation kinetics can be attributed to coupon-to-coupon variation in the number and width of the cracks. The temperature trends for C/SiC oxidation are somewhat different than observed for the carbon fiber constituent. The low temperature oxidation kinetics obtained at 816°C show the most rapid oxidation. In fact, complete consumption of the C fibers occurred in 0.5 atm O_2 in 25h as seen in both the weight loss results (Figure 10) and the polished cross-section of the post-test coupon shown in Figure 13. Note that the weight loss rate for the C/SiC coupons at this temperature scales with oxygen partial pressure just as it did for the C fibers in the crucible. The time for complete fiber oxidation has increased from approximately 1h for the fibers in the crucible (~0.5g) to about 20h for the fibers in the composite (~0.7g) presumably due to limited transport of oxidant through the cracks in the SiC seal coat.

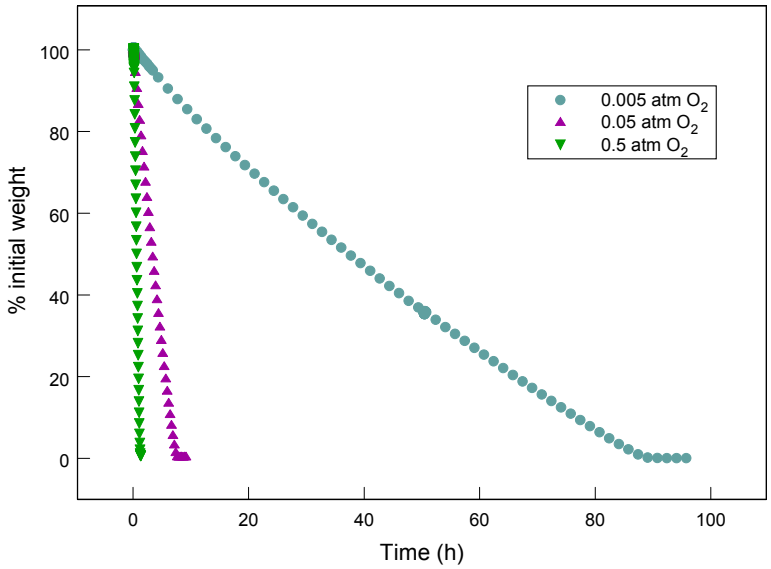

Figure 8. Oxygen partial pressure dependence of T-300 fiber oxidation weight change at 816°C.

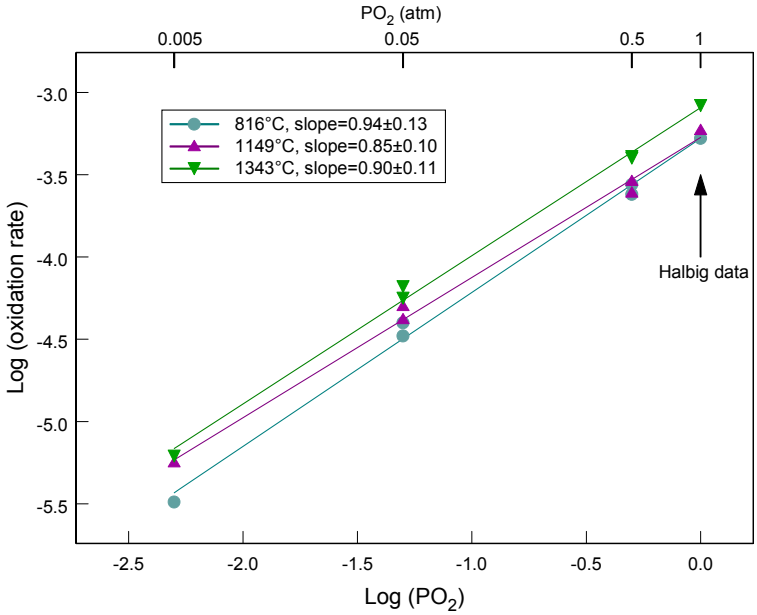

Figure 9. Oxygen partial pressure dependence of T-300 fiber oxidation rate.

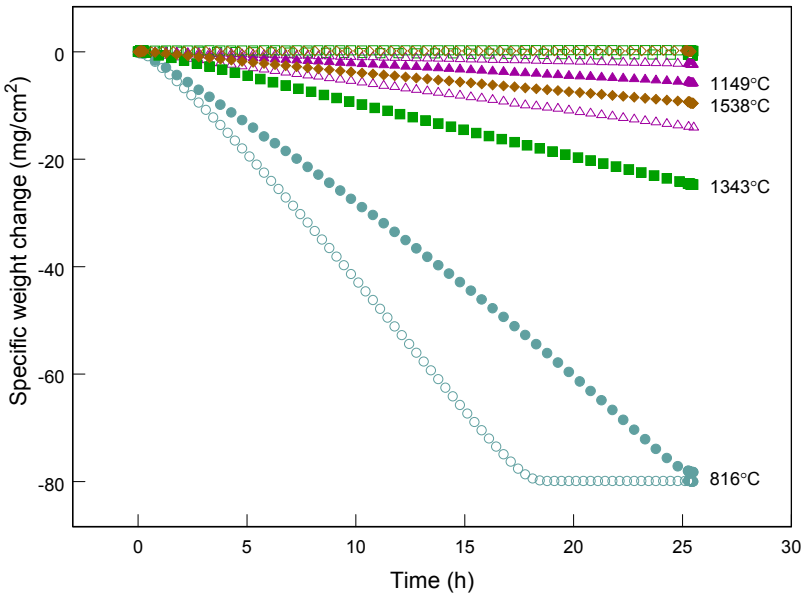

Figure 10. Oxidation weight loss of C/SiC composites in 100 ccm flowing 0.5 atm O_2/balance argon as a function of temperature.

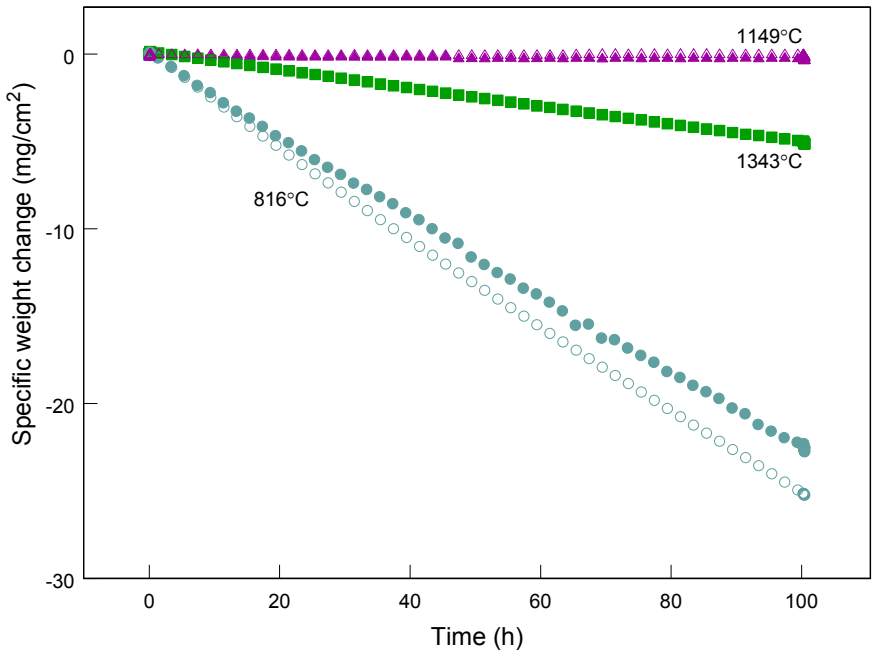

Figure 11. Oxidation weight loss of C/SiC composites in 100 ccm flowing 0.05 atm O_2/balance argon as a function of temperature.

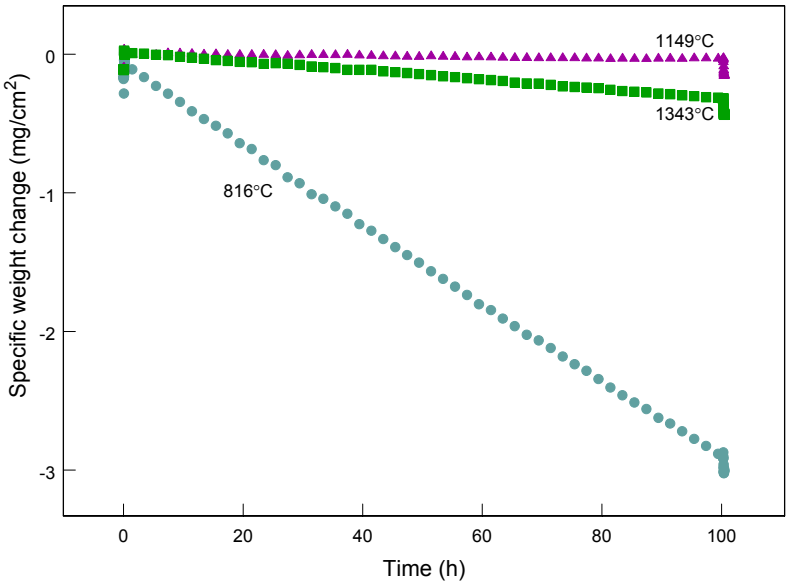

Figure 12. Oxidation weight loss of C/SiC composites in 100 ccm flowing 0.005 atm O_2/balance argon as a function of temperature.

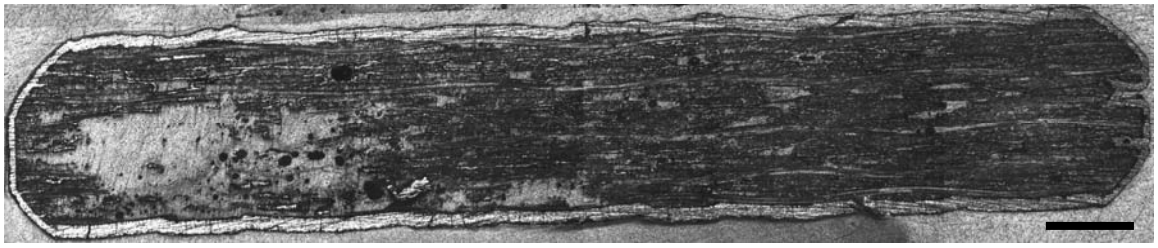

Figure 13. Polished cross-section of C/SiC composite coupon after exposure at 816°C in flowing (100 ccm) 0.5 atm O_2 for 25h. Note complete oxidation of T-300 fibers. Scale = 0.1 cm.

In contrast, a cross-section of the post 1538°C, 0.5 atm O_2, 25h exposure (Figure 14) shows little consumption of C fibers. The variability in results at the higher temperatures prevents any conclusive statements about temperature trends above 1100°C. However, the decreased rates observed at high temperatures relative to the 816°C can be explained several ways. First, oxidation of SiC is expected to occur at higher temperatures. The resulting growth of SiO_2 diminishes the crack width and thus lowers the rate of oxygen ingress. Second, the cracks should also begin to close as the temperature is increased due to thermal expansion of the SiC. Theoretically, the cracks should be closed at the original processing temperature.

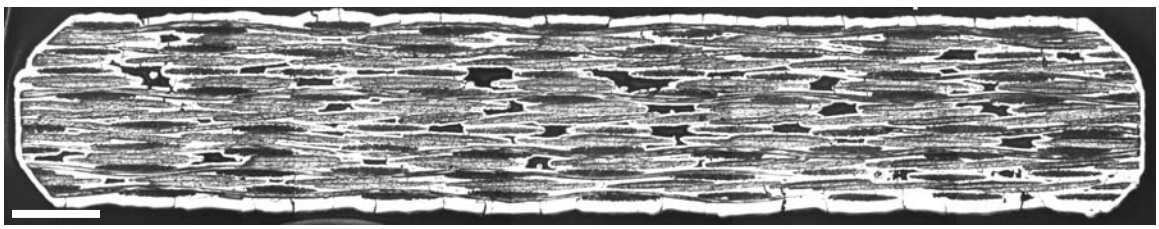

Figure 14. Polished cross-section of C/SiC composite coupon after exposure at 1538°C in flowing (100 ccm) 0.5 atm O_2 for 25h. Note minimal oxidation of T-300 fibers. Scale = 0.1 cm.

It is clear from the appearance of the coupons after the oxidation exposures that the SiC is oxidizing at temperatures of 1149°C and higher. As shown in Figure 15, interference colors are visible on the surface of the coupons indicating the formation of a thin oxide film. At higher temperatures the interference colors are no longer visible due to thickening of the oxide scale. SiC oxide thickness can be estimated from literature values for CVD SiC oxidation rates[15-16]. While these literature values were obtained in pure oxygen, the rates were estimated here assuming the oxidation rate is reduced in direct proportion with the oxygen pressure, i.e., the pressure dependence is given by P^n where n=1. This assumes oxidation is limited by transport of molecular oxygen through the growing silica scale, as was confirmed by Deal and Grove for the oxidation of silicon[17]. The estimated SiO_2 scale thickness for 25 and 100h exposures are listed as a function of oxygen partial pressure and temperature in Table 1.

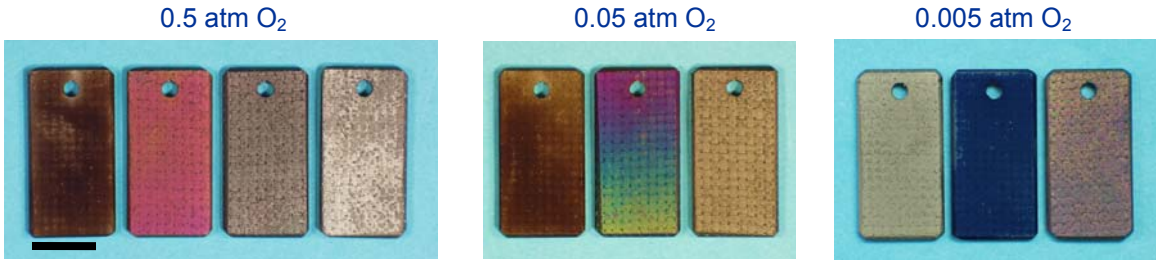

Figure 15. Macrophotos of C/SiC composite coupons after exposure for 25h in 0.5 atm O_2 and 100h in 0.05 and 0.005 atm O_2. The exposure temperatures at each oxygen partial pressure are (L to R) 816°, 1149°, 1343°, 1538°C. Note that no exposures were conducted at 1538°C in 0.05 and 0.005 atm oxygen partial pressure. Scale = 1 cm.

It can be seen that negligible oxide is expected to form at 816°C under any oxygen partial pressure condition. About one micron or less oxide is expected to form under even the highest temperature, high oxygen partial pressure conditions. It was difficult to observe any oxide film by SEM, however, a scale of about 1.5 μm was observed on a surface of the coupon exposed at 1538°C in 0.5 atm O_2. This is fairly consistent with the estimated oxide thickness reported in Table 1 for the same conditions.

Table 1. Estimated SiO_2 thickness (μm) for exposure of SiC as a function of temperature, oxygen partial pressure and time. Data interpolated/extrapolated from Ramberg[15](*) or Ogbuji[16](^).

PO_2, atm	Temperature, °C				Time, h
	816*	1149*	1343^	1538^	
0.5	0.024	0.428	0.741	1.173	25
0.05	0.010	0.253	0.468	0.742	100
0.005	0.001	0.055	0.148	0.235	100

Alternatively, crack closure can be explained by thermal expansion of the SiC seal coat. The distance between cracks in the SiC seal coat was measured for five coupons and was found to be 73 μm on average. Assuming a 73 μm segment of SiC expands according to published expression for $\Delta L/L_o$[18] then the average crack closure on heating can be estimated. These values are reported in Table 2. Table 3 compares the results from Tables 1 and 2 and summarizes which mechanism dominates crack closure as a function of oxygen partial pressure and temperature.

Table 2. Estimated crack closure due to SiC thermal expansion.
%ΔL/L from Touloukian[18].

T, °C	% ΔL/L	ΔL (μm) for 73 μm segment
816	0.376	0.275
1149	0.567	0.414
1343	0.685	0.500
1538	0.809	0.591

Table 3. Dominant mechanism for crack closure.
TE=thermal expansion. ox=SiC oxidation.

	Temperature, °C			
PO_2, atm	816	1149	1343	1538
0.5	TE	≈	ox	ox
0.05	TE	TE	≈	ox
0.005	TE	TE	TE	TE

The room temperature crack widths in the SiC seal coat were not measured statistically, however, cracks of about 1μm width are shown in Figure 16. Other cracks were significantly larger as shown in Figure 17. These crack widths are consistent the range of 0.5 to 3 μm crack widths measured by Lamouroux et al[4] for a similar SiC seal coat on a C/SiC composite.

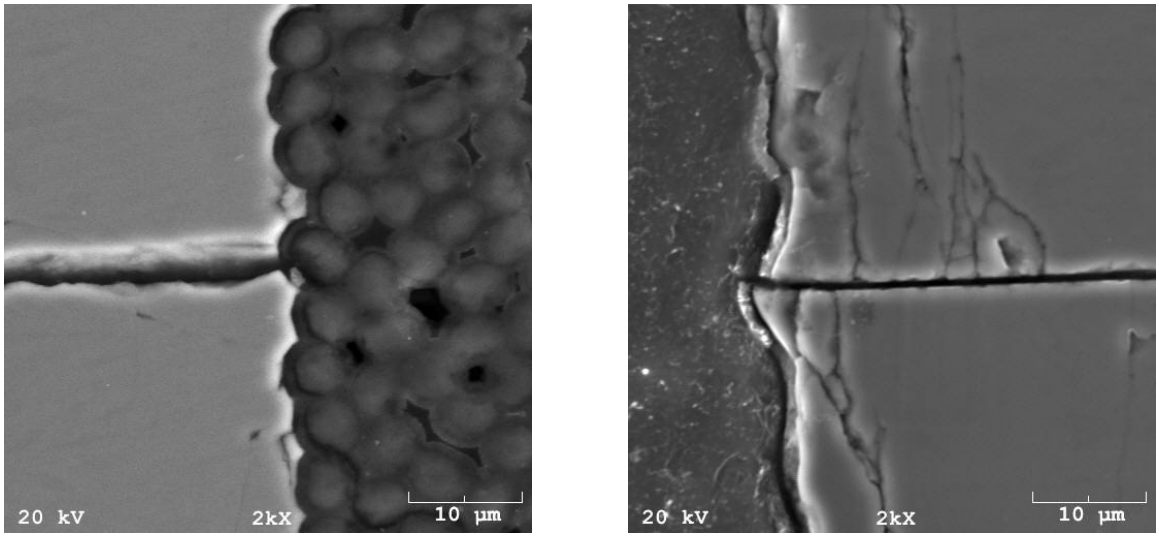

Figure 16. Cracks in SiC seal coat. Crack widths estimated to be approximately 1.1μm and 0.6 μm in the left and right photos respectively.

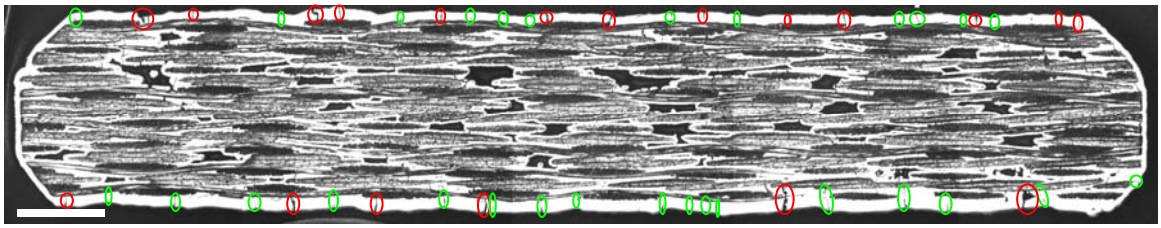

Figure 17. Highlighted cracks in SiC seal coat Green highlights indicate cracks on the order of 1 mm in width. Red highlights indicate larger cracks. The unmarked micrograph can be found in Figure 14. Scale = 0.1 cm.

In summary, several statements can be made regarding the oxidation of the C/SiC composites. SiC oxidation weight gains are negligible compared to C oxidation weight losses. It is unlikely that complete crack closure occurs in reduced oxygen partial pressure environments even at the highest temperatures, since weight loss is still observed and some of the cracks significantly exceed 1 μm in width. However, partial crack closure on heating can explain the decreased oxidation rates as the exposure temperature is increased. Since the coupon weight loss rates are reduced as the temperature increases in even the lowest oxygen partial pressures, it is likely that thermal expansion of the SiC rather than SiC oxidation dominates the crack closure.

SUMMARY AND CONCLUSIONS

T-300 fiber oxidation is gas phase diffusion limited in the temperature range between 816 and 1538°C. Oxidation kinetics are consistent with the predicted $T^{3/2}$ temperature dependence and pressure dependence for transport through a laminar boundary layer, P^n, with n=1. C/SiC oxidation kinetics were dominated by C fiber oxidation rather than SiC oxidation. Weight loss was observed at all temperatures between 816 and 1538°C and all oxygen partial pressures between 0.5 and 0.005 atm O_2. Rates were highest at 816°C and decreased at higher temperatures. The decreased oxidation rates at high temperature were attributed to closure of cracks in the SiC seal coat. A the low oxygen partial pressures in this study, the crack closure is more likely dominated by thermal expansion of the SiC rather than sealing of the cracks with SiO_2 from oxidation of SiC. Variability in coupon oxidation kinetics is attributed to variability in the number and width of cracks in the SiC seal coat.

REFERERNCES

1. I.M.K. Ismail, “On the Reactivity, Structure, and Porosity of Carbon Fibers and Fabrics,” Carbon 29 [6] 777-792 (1991).

2. F. Lamouroux, X. Bourrat, and R. Naslain, “Structure/Oxidation Behavior Relationship in the Carbonaceous Constituents of 2D-C/PyC/SiC Composites,” Carbon 31 [8] 1273-1288 (1993).

3. F. Lamouroux, G. Camus, J. Thebault, “Kinetics and Mechanism of 2D Woven C/SiC Composites: I, Experimental Approach,” J. Am. Ceram. Soc. 77 [8]2049-57 (1994).

4. F. Lamouroux, R. Naslain, J.-M. Jouin, “Kinetics and Mechanism of 2D Woven C/SiC Composites: II, Theoretical Approach,” J. Am. Ceram. Soc. 77 [8]2058-68 (1994).

5. M.C. Halbig, D.N. Brewer, and A.J. Eckel, “Degradation of Continuous Fiber Ceramic Matrix Composites Under Constant Load Conditions,” NASA TM-2000-209681.

6. R.M. Sullivan, “A model for the oxidation of carbon silicon carbide composite structures,” Carbon 43, 275-285 (2005).

7. E.J. Opila, “Oxidation of T-300 Carbon Fibers in Water Vapor Environments,” pp. 159-168 in High Temperature Corrosion and Materials Chemistry III, eds. M. McNallan and E.Opila, the Electrochemical Society, Pennington, NJ, 2001.

8. M.J. Verrilli, E.J. Opila, A. Calomino, J.D. Kiser, “Effect of Environment on the Stress-Rupture Behavior of a Carbon-Fiber-Reinforced Silicon Carbide Ceramic Matrix Composite,” J. Am. Ceram. Soc. 87 [8] 1536-1542 (2004).

9. P.L. Walker, Jr., F. Rusinko, Jr., and L.G. Austin, “Gas Reactions of Carbon,” Adv. Catal., Vol. XI, 133-221 (1959).

10. E.A. Gulbransen, K.F. Andrew, and F.A. Brassart, “The Oxidation of Graphite at Temperatures of 600° to 1500°C and at Pressures of 2 to 76 Torr of Oxygen,” J. Electrochem. Soc. 110 [6] 476-483 (1963).

11. J. Podhiny, B.J. Sullivan, K.S. Bey, E. Opila, J. Serra, R. Sullivan, “Development and Preliminary TGA Correlation Results of a Finite Element Based Durability Model for CMCs,” Proceedings of JANNAF Hypersonic Materials: TPS and Hot Structures, 32nd Annual Conference on Composites, Materials, and Structures, January 29, 2008.

12. E.J. Opila, "The Influence of Alumina Reaction Tube Impurities on the Oxidation of CVD SiC," J. Am. Cer. Soc., 78 [4] 1107-10 (1995).

13. G.H. Geiger and D.R. Poirier, p. 464 in Transport Phenomena in Metallurgy, Addison-Wesley Publishing Company, Reading, MA, 1973.

14. Ibid. pp. 525-537.

15. C.E. Ramberg, G. Cruciani, K.E. Spear, R.E. Tressler, C.F. Ramberg, “Passive-Oxidation Kinetics of High Purity Silicon Carbide from 800° to 1100°C,” J. Am. Ceram. Soc. 79 [11] 2897-2911 (1996).

16. L.U.J.T. Ogbuji, E.J. Opila, “A Comparison of the Oxidation Kinetics of SiC and Si_3N_4,” J. Electrochem. Soc. 142 [3] 925-930 (1995).

17. B.E. Deal, A.S Grove, “General Relationship for the Thermal Oxidation of Silicon,” J. Appl. Phys. 36 [12] 3770-3778 (1965)

18. Y.S. Touloukian, R.K. Kirby, R.E. Taylor, T.Y.R Lee, p. 873 in Thermophysical Properties of Matter, Vol. 13, Thermal Expansion - Nonmetallic Solids, IFI Plenum, New York, 1977.